PROCEEDINGS OF SCIENCE

Electroweak penguins at LHCb

Samuel Coquereau[∗†]
LPNHE, Université Pierre et Marie Curie, Université Paris Diderot, CNRS/IN2P3, Paris (France)
E-mail: samuel.coquereau@cern.ch

Decays proceeding via electroweak penguins decays are excellent probes to search for new effects beyond the Standard Model (SM). The $b \to s\ell\ell$ processes are particularly interesting since they give access to many observables (branching fractions, asymmetries, angular observables) sensitive to contributions beyond the SM. Latest results of the $b \to s\ell\ell$ decays, obtained with the LHCb experiment, will be presented in these proceedings.

The European Physical Society Conference on High Energy Physics
22-29 July 2015
Vienna, Austria

∗Speaker.
†On behalf of the LHCb collaboration.

PoS(EPS-HEP2015)535

1. Introduction

Flavour changing neutral current (FCNC) decays are, in the SM, rare, as they are forbidden at tree level and proceed through loop-order Feynman diagrams. New particles can appear in the loop, leading to additional Feynman diagrams that can affect the branching fraction and the angular distribution of the final state particles. Electroweak penguins decays are important tools to searches for physics beyond the SM. Latest results of the $b \to s\ell\ell$ decays, obtained with the full Run I data sample collected by the LHCb experiment, will be presented in these proceedings.

2. Branching fraction of $B^0_{(s)} \to \pi^+\pi^-\mu^+\mu^-$

Both the B^0 and B^0_s meson can decay into the same $\pi^+\pi^-\mu^+\mu^-$ final state. The B^0 proceed via the $b \to d\mu^+\mu^-$ transition and mainly by the decay $B^0 \to \rho^0\mu^+\mu^-$, while the B^0_s mesons decay via the $b \to s\mu^+\mu^-$ transition and the decay $B^0_s \to f^0(980)\mu^+\mu^-$. The $b \to d$ transitions are predicted, in the SM, to be suppressed by the factor $|\frac{V_{td}}{V_{ts}}|^2 \sim 0.04$ with respect to the $b \to s$ decays.

The decays $B^0_{(s)} \to \pi^+\pi^-\mu^+\mu^-$ have been studied [1] with the full Run I dataset, corresponding to $3fb^{-1}$ of integrated luminosity collected by the LHCb experiment in 2011 and 2012. The invariant mass of the pion pairs is set to be in the range 0.5-1.3 GeV/c^2 including both ρ^0 and $f^0(980)$ resonances. The mass model has been validated using the invariant mass distribution of the $\pi^+\pi^-\mu^+\mu^-$ final state in the control channels, the $B^0_{(s)} \to J/\psi\pi^+\pi^-$ decays. The invariant mass of the $\pi^+\pi^-\mu^+\mu^-$ distribution for the signal decays, $B^0_{(s)} \to \pi^+\pi^-\mu^+\mu^-$, as well as the control channels, $B^0_{(s)} \to J/\psi\pi^+\pi^-$, can be seen in Figure 1. The signal yields are found to be $40 \pm 10 \pm 3$ for the $B^0 \to \pi^+\pi^-\mu^+\mu^-$ decay and $55 \pm 10 \pm 5$ for the decay $B^0_s \to \pi^+\pi^-\mu^+\mu^-$, corresponding to a significance of 4.8σ and 7.2σ respectively. The branching fractions, determined with respect to the normalization channel, the decay $B^0_{(s)} \to J/\psi K^*(982)^0$, are found to be

$$\mathscr{B}(B^0 \to \pi^+\pi^-\mu^+\mu^-) = (2.11 \pm 0.51(\text{stat}) \pm 0.15(\text{syst}) \pm 0.16(\text{norm})) \times 10^{-8},$$
$$\mathscr{B}(B^0_s \to \pi^+\pi^-\mu^+\mu^-) = (8.6 \pm 1.5(\text{stat}) \pm 0.7(\text{syst}) \pm 0.7(\text{norm})) \times 10^{-8},$$

These value are in good agreement with the SM predictions.

3. Angular analysis of the decay $B^0 \to K^{*0}\mu^+\mu^-$

The rare decay $B^0 \to K^{*0}\mu^+\mu^-$ is interesting since it allows to access to many angular observables sensitive ti NP contributions. The $K^+\pi^-\mu^+\mu^-$ final state can be fully described by three decay angles $\vec{\Omega} = (\cos\theta_l, \cos\theta_K, \phi)$ and the invariant mass of the dilepton system squared, q^2. The CP-average angular distribution of the decay $B^0 \to K^{*0}\mu^+\mu^-$ is written as

$$\begin{aligned}
\frac{1}{\mathrm{d}(\Gamma+\bar{\Gamma})/\mathrm{d}q^2}\frac{\mathrm{d}^3(\Gamma+\bar{\Gamma})}{\mathrm{d}\vec{\Omega}} = \frac{9}{32\pi}\Big[&\frac{3}{4}(1-F_\mathrm{L})\sin^2\theta_K + F_\mathrm{L}\cos^2\theta_K + \frac{1}{4}(1-F_\mathrm{L})\sin^2\theta_K\cos 2\theta_\ell \\
&-F_\mathrm{L}\cos^2\theta_K\cos 2\theta_\ell + S_3\sin^2\theta_K\sin^2\theta_\ell\cos 2\phi + S_4\sin 2\theta_K\sin 2\theta_\ell\cos\phi \\
&+S_5\sin 2\theta_K\sin\theta_\ell\cos\phi + \frac{4}{3}A_\mathrm{FB}\sin^2\theta_K\cos\theta_\ell + S_7\sin 2\theta_K\sin\theta_\ell\sin\phi \\
&+S_8\sin 2\theta_K\sin 2\theta_\ell\sin\phi + S_9\sin^2\theta_K\sin^2\theta_\ell\sin 2\phi\Big].
\end{aligned}$$

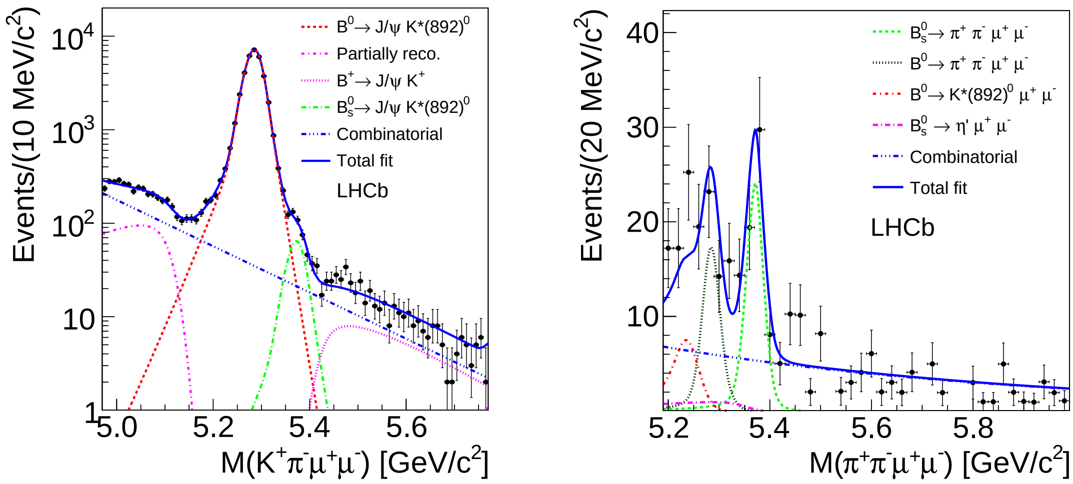

Figure 1: $\pi^+\pi^-\mu^+\mu^-$ invariant mass distributions for the control channel $B^0_{(s)} \to J/\psi\pi^+\pi^-$ (left) and for the signal decays, $B^0_{(s)} \to \pi^+\pi^-\mu^+\mu^-$ (right)

Here the angular observables $F_{\rm L}$, $A_{\rm FB}$ and S_i are bilinear combinations of six complex amplitudes $\mathscr{A}^{\rm L,R}_{0,\|,\perp}$ corresponding to different transversity states of the K^{*0} and the different chiralities of the dimuon system. The measurement of the less form-factor dependent observable $P_5' = \frac{S_5}{\sqrt{F_{\rm L}(1-F_{\rm L})}}$, proposed in Ref. [2], has also been realized.

An update of the angular analysis of $B^0 \to K^{*0}\mu^+\mu^-$ using the full Run I data sample corresponding to 3 fb^{-1} is presented Ref. [3] . For the first time the complete set of *CP*-averaged observables has been extracted. The selection of $B^0 \to K^{*0}\mu^+\mu^-$ signal candidates is improved compared to Ref. [4, 5] with more stringent vetoes to reject peaking backgrounds and with a more efficient but simpler multivariate classifier to reduce the combinatorial background. The distribution of q^2 as function of the invariant mass of the $K^+\pi^-\mu^+\mu^-$ final state after the full selection can be see in Figure 2. The q^2 regions $8.0 < q^2 < 11.0$ GeV^2/c^4 and $12.5 < q^2 < 15.0$ GeV^2/c^4 contain the tree-level decays $B^0 \to J/\psi(\to \mu^+\mu^-)K^{*0}$ and $B^0 \to \psi(2S)(\to \mu^+\mu^-)K^{*0}$ respectively, which are used as control channels. A clear $B^0 \to K^{*0}\mu^+\mu^-$ signal is visible as a vertical band in Fig. 2 and the signal yield integrated over q^2 is 2398 ± 57.

The analysis is performed in different bins of q^2, where the angular observables are determined by an unbinned maximum likelihood fit to the distribution of the $K^+\pi^-\mu^+\mu^-$ invariant mass, the $K^+\pi^-$ mass and the three angles. Since no angular foldings have been applied, the correlation matrices between the observables are also provided, which is important for the use of the results in global fits. To constrain the contribution from events with a spin-0 configuration in the $K^+\pi^-$ system, the S-wave, a simultaneous fit of the $K^+\pi^-$ invariant mass distribution is performed.

The results of the observables $F_{\rm L}$, $A_{\rm FB}$ and P_5' are shown in Fig. 3 and Fig. 4 respectively, with the SM prediction from Ref. [6, 7] and Ref. [8]. Both $F_{\rm L}$ and $A_{\rm FB}$ agree with SM predictions, while the less form-factor dependent observable P_5' is measured to be above the SM prediction Ref. [8] between 4 and 8 GeV^2/c^4. This results is compatible with the previous measurement [5] and corresponds to a deviation of 2.9σ in the q^2 bins, [4.0-6.0] GeV^2/c^4 and [6.0-8.0] GeV^2/c^4.

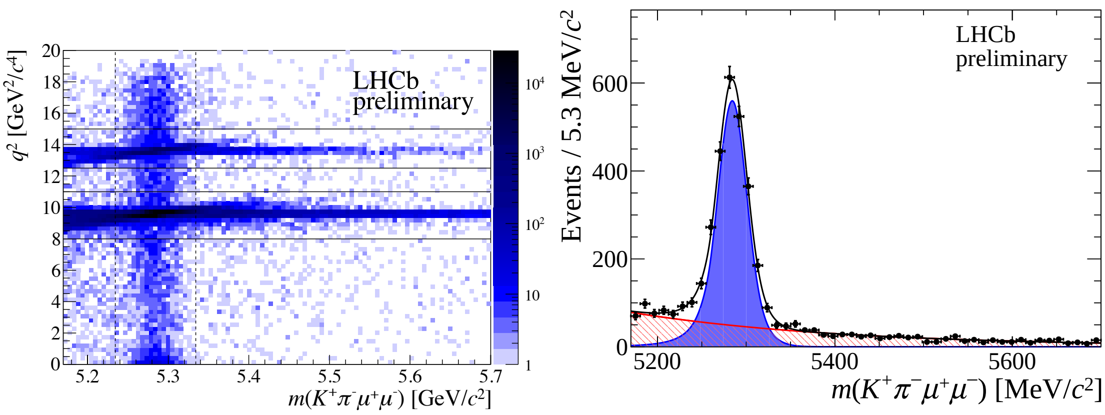

Figure 2: q^2 as function of the invariant mass of the $K^+\pi^-\mu^+\mu^-$ final state (left). Invariant mass of the $B^0 \to K^{*0}\mu^+\mu^-$ signal decay integrated over the full q^2 range (right).

The other observables, S_{3-9}, are in good agreement with SM prediction.

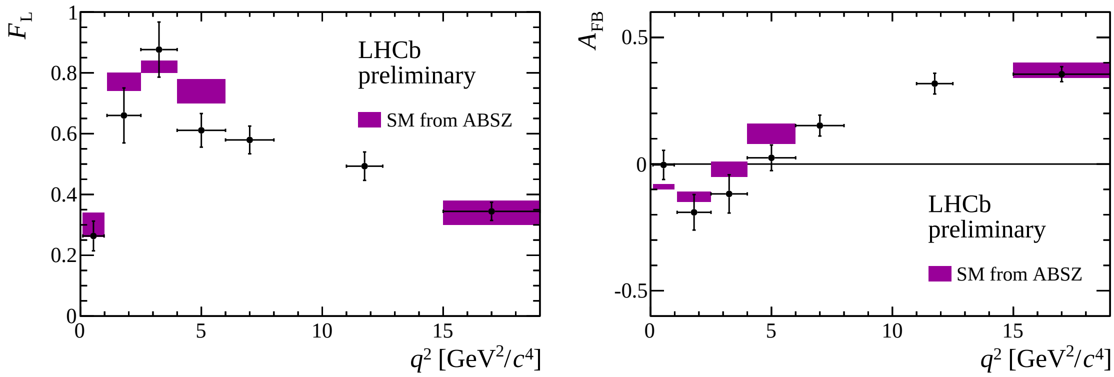

Figure 3: The angular observables F_L, A_{FB}, overlaid with the SM prediction from [6, 7]

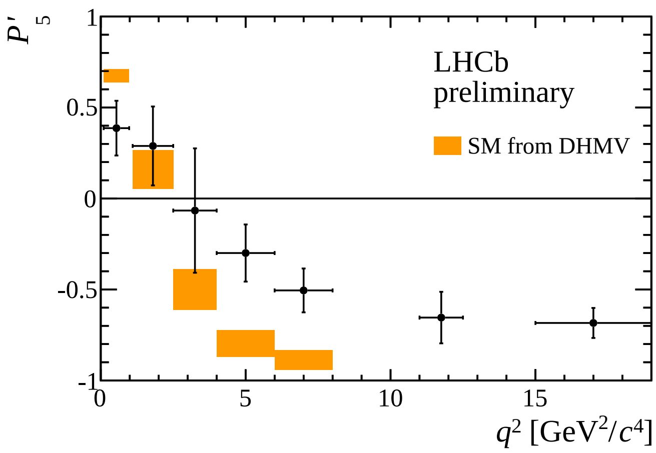

Figure 4: The angular observables P'_5 overlaid with the SM prediction from [8]

4. Branching fraction and angular analysis of the rare decay $B_s^0 \to \phi\mu^+\mu^-$

The decay $B_s^0 \to \phi(\to K^+K^-)\mu^+\mu^-$ is related to the decay $B^0 \to K^{*0}\mu^+\mu^-$, which has been presented above. The B_s^0 meson production is suppressed by $\sim 3/16$ with respect to the B^0 meson, due to the fragmentation fraction ratio f_s/f_d and including the ratio $\mathcal{B}(\phi \to K^+K^-)/\mathcal{B}(K^{*0} \to K^+\pi^-)$. The ϕ resonance is narrower than the K^{*0} resonance, allowing a clean selection with a small background level. The measurement of the branching fraction and the angular analysis of the decay $B_s^0 \to \phi\mu^+\mu^-$ are presented in Ref. [9]. The distribution of q^2 as function of the invariant mass of the $K^+K^-\mu^+\mu^-$ final state after the full selection is shown in Fig. 5 and the signal yield integrated over the full range of q^2 is found to be 432 ± 24.

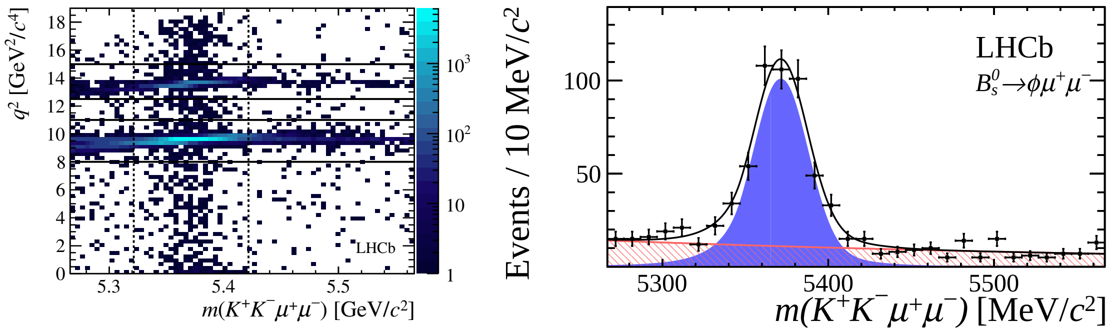

Figure 5: q^2 as function of the invariant mass of the $K^+K^-\mu^+\mu^-$ final state (left). Invariant mass of the $B^0 \to \phi\mu^+\mu^-$ signal decay integrated over the full q^2 range (right).

The differential branching fraction in a given q^2 bin $[q^2_{\min}, q^2_{\max}]$ is determined according to:

$$\frac{\mathrm{d}\mathcal{B}(B_s^0 \to \phi\mu^+\mu^-)}{\mathrm{d}q^2} = \frac{1}{q^2_{\max} - q^2_{\min}} \cdot \frac{N_{\phi\mu\mu}}{N_{J/\psi\phi}} \cdot \frac{\varepsilon_{J/\psi\phi}}{\varepsilon_{\phi\mu\mu}} \cdot \mathcal{B}(B_s^0 \to J/\psi\phi)\mathcal{B}(J/\psi \to \mu^+\mu^-),$$

were $N_{\phi\mu\mu}$ and $N_{J/\psi\phi}$ are the yield of the signal and normalisation mode and $\varepsilon_{\phi\mu\mu}$ and $\varepsilon_{J/\psi\phi}$ their respective efficiencies. The total branching fraction is found to be $\mathcal{B}(B_s^0 \to \phi\mu^+\mu^-) = (7.97^{+0.45}_{-0.43} \pm 0.22 \pm 0.23 \pm 0.60) \times 10^{-7}$ and the differential branching fraction is shown in Fig. 6. For the q^2 region $1.0 < q^2 < 6.0\ \mathrm{GeV}^2/\mathrm{c}^4$ the differential branching fraction of $(2.58^{+0.33}_{-0.31} \pm 0.08 \pm 0.19) \times 10^{-8}\mathrm{GeV}^{-2}/\mathrm{c}^4$ is 3.3σ below the SM prediction [6, 7] of $(4.81 \pm 0.56) \times 10^{-8}\ \mathrm{GeV}^{-2}/\mathrm{c}^4$.

Since the $K^+K^-\mu^+\mu^-$ final state is not flavour specific, the only angular observables accessible in the decay $B_s^0 \to \phi\mu^+\mu^-$ are the CP-averages $F_{\mathrm{L}}, S_{3,4,7}$ and the CP asymmetries $A_{5,6,8,9}$. The flavour-averaged differential decay rate, as a function of the decay angles in bins of q^2, is given by

$$\begin{aligned}\frac{1}{\mathrm{d}\Gamma/\mathrm{d}q^2}\frac{\mathrm{d}^3\Gamma}{\mathrm{d}\vec{\Omega}} = \frac{9}{32\pi}\Big[&\frac{3}{4}(1-F_{\mathrm{L}})\sin^2\theta_K + F_{\mathrm{L}}\cos^2\theta_K + \frac{1}{4}(1-F_{\mathrm{L}})\sin^2\theta_K\cos 2\theta_\ell \\ &- F_{\mathrm{L}}\cos^2\theta_K\cos 2\theta_\ell + S_3\sin^2\theta_K\sin^2\theta_\ell\cos 2\phi + S_4\sin 2\theta_K\sin 2\theta_\ell\cos\phi \\ &+ A_5\sin 2\theta_K\sin\theta_\ell\cos\phi + A_6\sin^2\theta_K\cos\theta_\ell + S_7\sin 2\theta_K\sin\theta_\ell\sin\phi \\ &+ A_8\sin 2\theta_K\sin 2\theta_\ell\sin\phi + A_9\sin^2\theta_K\sin^2\theta_\ell\sin 2\phi\Big].\end{aligned}$$

The angular observables are determined by an unbinned maximum likelihood fit to the $K^+K^-\mu^+\mu^-$ invariant mass distribution and the three angular distribution in each q^2 bin. The angular observables are found to be in good agreement with the SM predictions and the angular observables $F_{\rm L}$ is shown in Fig. 6.

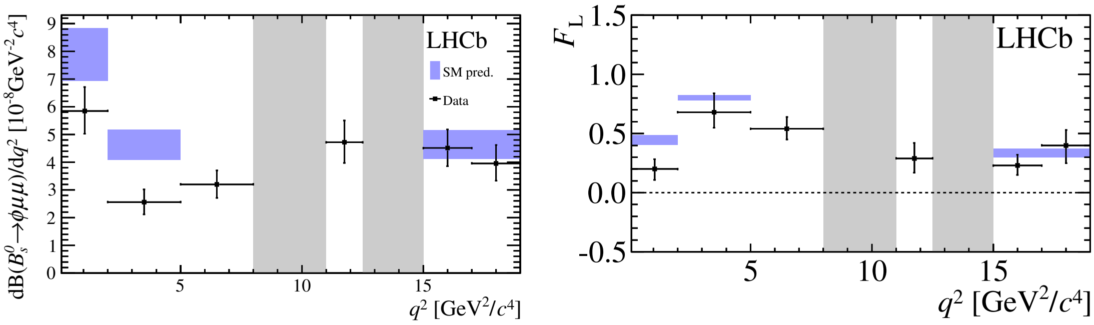

Figure 6: Differential branching fraction of the decay $B_s^0 \to \phi\mu^+\mu^+$ (left). CP-averaged angular observable $F_{\rm L}$ shown by black dots (right). Overlaid are the SM predictions [6, 7] indicated by blue shaded boxes. The vetoes excluding the charmonium resonances are indicated by grey areas.

5. Conclusion

The measurement of observables in the rare decays agree in general with the SM predictions. However some deviations are observed, the branching fraction of the $B_s^0 \to \phi\mu^+\mu^-$ decay is 3.3σ lower than SM prediction in the q^2 bin $1 < q^2 < 6$ GeV^2/c^4 and the updated angular analysis of the decay $B^0 \to K^{*0}\mu^+\mu^-$ finds local deviations corresponding to 2.9σ from the SM prediction in each of the two q^2 bins $4 < q^2 < 6$ GeV^2/c^4 and $6 < q^2 < 8$ GeV^2/c^4.

References

[1] LHCb Collaboration, R. Aaij *et al.*, Phys. Lett. B **743** (2015) 46 [arXiv:1412.6433 [hep-ex]].

[2] S. Descotes-Genon*et al.*, JHEP **1305** (2013) 137 [arXiv:1303.5794 [hep-ph]]

[3] LHCb Collaboration, R. Aaij *et al.*, LHCb-CONF-2015-002, cds.cern.ch/record/2002772.

[4] LHCb Collaboration, R. Aaij *et al.*, JHEP **1308** (2013) 131 [arXiv:1304.6425 [hep-ex]]

[5] LHCb Collaboration, R. Aaij *et al.*, Phys. Rev. Lett. **111** (2013) 191801 [arXiv:1308.1707 [hep-ex]]

[6] W. Altmannshofer and D. M. Straub, Eur. Phys. J. C **75** (2015) 382 [arXiv:1411.3161 [hep-ph]]

[7] A. Barucha, D. M. Straub and R. Zwicky [arXiv:1503.05534 [hep-ex]]

[8] S. Descotes-Genon *et al.*, JHEP **1412** (2014) 125 [arXiv:1407.8526 [hep-ph]]

[9] LHCb Collaboration, R. Aaij *et al.*, JHEP **1509** (2015) 179 [arXiv:1506.08777 [hep-ex]]